

Digital Reconstruction of Ancient Paper Artifacts

Ivan Gerace(✉)

Laboratorio di Matematica Computazionale "Sauro Tulipani" Dipartimento di Matematica e Informatica, Universitá degli Studi di Perugia, Perugia, Italy
ivan.gerace@unipg.it

Abstract. This work deals with the digital reconstruction of ancient playing cards. We divide the reconstruction process into several phases: color balancing and homogenization, outer contour detection and regularization, and final data fitting. We propose regularization techniques to address some of these challenges. In particular, the regularization method we developed for contour restoration has novel smoothness terms. We have successfully reconstructed some ancient cards, and the quality of these reconstructions confirms the effectiveness of our proposed technique.

Keywords: defading problem · deblurring · regularization techniques · contour detection · document reconstruction

1 Introduction

Many books have been written about the history of playing cards, but they have never indisputably clarified their origins [8,22,24,29]. However, playing cards spread widely in Europe starting from the 14th century. During the 20th century, the international standard deck, such as the English type, was established; nevertheless, in different countries, various types of cards are still in use to allow the playing of local games. However, some of these card types have disappeared, and only a few decks have survived. These decks tell the local history of a population and are highly sought after by collectors [28,29]. Nevertheless, the images of these decks are deteriorated because of the ancient printing techniques and the degradation suffered by the paper over time. In this paper, we present a digital restoration technique that allows the reconstruction of an ancient deck of cards that preserves the original artistic style and provides for a new reprint. In particular, we are interested in the reconstruction of the ancient *Perugine* playing cards.

We divide the reconstruction of the card deck into several phases. In the first phase, we address the damage caused by the deterioration of the paper and printing inks. The data we are examining consists of a set of faded images [7,15,30,31]. Using uniform color spaces can be beneficial for restoring faded images [11]. In such spaces, adjacent colors appear similar to the human eye, often incorporating

© The Author(s), under exclusive license to Springer Nature Switzerland AG 2026
O. Gervasi et al. (Eds.): ICCSA 2025 Workshops, LNCS 15892, pp. 400–416, 2026.
https://doi.org/10.1007/978-3-031-97638-4_25

one component related to luminance and another related to chrominance (see also [10,19]). This paper utilizes the recently proposed QTLC-r^*g^* (*Quadratically Transformed Luminance Chrominance-*r^*g^*) space, as introduced in [11]. This space possesses reconstruction characteristics akin to the CIE $L^*a^*b^*$ color space and maintains a quadratic transformation between itself and RGB space. A defading technique that employs this color space has already been proposed in [11]. This technique includes a deblurring phase to reconstruct the diffusion of color hues over time. In this paper, we revisit this technique and determine the optimal parameters for reconstructing the analyzed deck. The second phase involves restoring the proper separation of colors using border lines. The playing cards' images feature color areas enclosed by black borders. These borders are designed to contain the objects being represented fully. However, in the data being analyzed, some of these lines are occasionally disrupted due to the printing techniques used, causing some colors to appear as if they are spilling out of the borders. This problem can be classified as a curve reconstruction problem (see also [9,25]). This paper does not address these issues and will reserve them for further study. The third phase involves a new reconstruction to remove artifacts and enhance color homogeneity. The accurate reconstruction of edges from the previous phase supports this new process. We addressed this issue using a regularization technique [14,17]. Throughout this phase, we continued to use the QTLC-r^*g^* color space, which provides better stability against color variations. The fourth phase involves detecting the external contour. Due to the printing technique, the ideal contour is not explicitly present in the data and must be accurately estimated. We divide this phase into two sub-phases: In the first sub-phase, we implement fast routines to eliminate evident defects in the estimated contour. The second sub-phase distinguishes the outer and inner borders and any black lines in the drawing. The subsequent phase is the regularization of the obtained border. We propose to address this phase using a novel regularization technique. We define the reconstructed contour based on an appropriate energy function composed of three terms: the first term is a consistency term that ensures we do not deviate significantly from the previously estimated border; the second term regulates the length of the border; and the third term measures its thickness. We employ a simulated annealing algorithm to minimize the defined energy function [21]. The estimated border does not align with the estimated image. Thus, the final phase finds the color intensities where the color remains undefined. This issue represents a classic sparse data problem [20]. We propose a regularization technique to estimate the missing values.

The paper is organized as follows: Sect. 2 outlines the reasons for selecting the deck of cards to be reconstructed. In Sect. 3, the defading technique is presented. In Sect. 4, the proposed color uniform technique is exposed. Section 5 proposes a method for determining the external edge, while the regularization of this edge is analyzed in Sect. 6. Finally, Sect. 7 presents a technique for adapting the reconstructed image to the new edge. At the end of each section, the relative experimental results are presented.

2 Deck of Cards Under Reconstruction

Evidence of the use of playing cards in the area of Perugia, located in central Italy, dates back to the 15th century [36]. In particular, we can mention a deck of that time found in Assisi, about 20 km from Perugia [34], the sheet of playing cards found in a book printed in Perugia from the early 1500 s [35], and the comedy *Gioco de trionfi, che fanno quattro compagni, detti Delio, Timbreo, Castalio, e Caballino* printed in Perugia in 1521 which has the tarot as its subject [33].

In the second half of the 19th century, different types of playing cards were already widespread in Italy. This diversity was mainly due to the tax policy on the sale of cards in the various pre-unification states. Even after the Kingdom of Italy was established in 1861, the types of decks of cards in use reflected the previously existing division. A particular situation occurred in the territories of the former Papal States, where Perugia was located. In these areas, an actual local standard deck had not been created, but in addition to using the Piacenza deck of cards, there was the diffusion of different types of cards. In this paper, we restore one of the desks. In particular, in the former Papal States, playing cards vary slowly from the *Romagnale* to the deck in question and the *Viterbese* one (see Fig. 1).



(a) (b) (c)

Fig. 1. (a): *Romagnale* cards produced by Murari (from Gerace's private collection); (b): *Perugine* cards produced by Murari (from Museo civico di Bari); (c): *Viterbesi* cards produced by Murari (from Gerace's private collection).

The deck in question had an initial diffusion of sales thanks to the Murari company of Bari. However, the official type of this deck of cards produced by Murari is unknown. The Murari company ceased its activities in 1929. The well-known writer and collector Sylvia Mann describes the type of a deck of cards

similar to the one shown in Fig. 1 (b), produced by the Ambrosi company of Padova, as *Romagnole II* [28]. The same type of cards was made locally by the Bartolini company of Perugia, as seen from the image of the ace of coins available online [39]. This card is similar to the ace of coins that appears in Fig. 1 (b). It differs only in the presence of the stamp duty of the period 1874–1879 and the manufacturing company's name. The Bartolini company was active in Perugia in the late nineteenth as can be seen from some extracts of the *Annuario d'Italia* in the pages relating to manufacturers in Perugia (see Fig. 2).

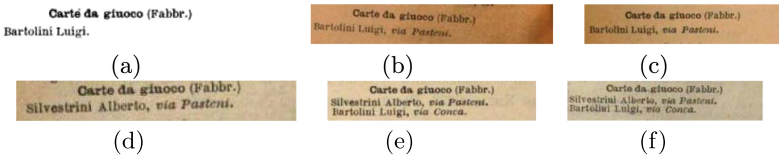

Fig. 2. Extracts of the *Annuario d'Italia* of manufacturers in Perugia of the year (a): 1889 [1]; (b) 1892 [2]; (c) 1893 [3]; (d) 1894 [4]; (e) 1896 [5]; (f) 1899 [6].

The Solesio company of Genoa later produced the same type of cards (See Fig. 3 (c)). This company has not been active since 1960, and the remaining decks of cards of this type are extremely rare. However, the paper wrapper in Fig. 3 (b) is attributed to this deck. This wrapper bears the writing *Tipo Perugia*. In particular, [16] says that a deck produced by Solosio of such cards with the relative wrapper belongs to Romano Biani's private collection. Furthermore, a comparative study reported on [16] states that the type of cards examined differs substantially from the *Romagnole*. In particular, [16] says that due to the posture of the figures, the length of the kings' robes, and the characteristics of the ace of coins, the cards in question differ from other classic Italian patterns and probably define a new one. So, in this paper, we consider the type of cards in question as *Perugine*. In Perugia, using the *Piacentine* deck of cards for playing local games is widespread (see Fig. 4 (a)). However, it would be interesting to revive the use of the local ancient deck, which probably was historically used until the early twentieth century. To this end, this paper analyze the reconstruction of a deck of cards of this type from images of Virgilio Ferrari's private collection (see Fig. 3 (c)).

3 Defading Phase

The data under examination are faded, noisy, and blurry. A first defading phase is, therefore, necessary. This problem has been successfully addressed in [11] by using a new uniform color space, the QTLC-r^*g^* (*Quadratically Transformed Luminance Chrominance-*r^*g^*) space. This space appears to have reconstruction properties similar to $L^*a^*b^*$ despite having a simple coordinate change with the



(a) (b) (c)

Fig. 3. (a): Ace of coins produced by the Bartolini company [39]; (b): Playing card wrapper by the Solesio company; (c) *Perugine* playing cards produced by the Solesio company (from Ferrari's private collection).

RBG space. In particular, given a color represented by the triple $(r, g, b) \in [0, 1]^3$ in the Adobe RGB space, we obtain

$$\begin{cases} l = (1/4)r + (1/2)g + (1/4)b, \\ r^* = \dfrac{r-l}{l}, \qquad g^* = \dfrac{g-l}{l}, \end{cases}$$

where l is the luminance coordinate of the color in the QTLC-r_*g_* space, while the chrominance coordinates are given by

$$\begin{cases} \alpha = (5/8)r^* - (3/8)g^* + (1/4)\, r^*\, g^* \\ \beta = (3/8)r^* + (5/8)g^*. \end{cases}$$

If we consider the image in Fig. 4 (a), Fig. 4 (b) shows its luminance; Fig. 4 (c) presents its chrominance; while, the component α and β are shown in Fig. 4 (d), and (e), respectively.

The defading method proposed in [11] is divided into two phases: The first phase involves manipulating contrast and hue, while the second involves denoising and deblurring. Let $x^{(0)} = (\mathbf{l}^{(0)}, \boldsymbol{\alpha}^{(0)}, \boldsymbol{\beta}^{(0)}) \in \mathbb{R}^{n\times m\times 3}$ be the $n \times m$ faded image, where $(\mathbf{l}^{(0)}, \boldsymbol{\alpha}^{(0)}, \boldsymbol{\beta}^{(0)})$ are, respectively, the vectors in lexicographic form of the luminance, α-chrominance and β-chrominance. The first phase is quite immediate: After establishing the values $l_0, \alpha_0^+, \beta_0^+ > 0$ and $\alpha_0^-, \beta_0^- < 0$, which we want to keep constant, the color values for each pixel (i, j) are determined



(a) (b) (c) (d) (e)

Fig. 4. (a): Full-figure King of Coins of the *Piacentine* desk produced by Dal Negro (from Gerace's private collection); (b): The luminance component; (c): The chrominance component with constant luminance equal to 180; (d) The α component; (e) The β component.

as follows.

$$
\begin{aligned}
l_{i,j}^{(1)} &= (c_l(l_{i,j}^{(0)} - l_0) + l_0)^{(+)}, \\
\alpha_{i,j}^{(1)} &= \begin{cases} (c_\alpha^+(\alpha_{i,j}^{(0)} - l_\alpha^+) + l_\alpha^+)^{(+)} \text{ if } \alpha_{i,j} \geq 0, \\ (c_\alpha^-(\alpha_{i,j}^{(0)} - l_\alpha^-) + l_\alpha^-)^{(-)} \text{ if } \alpha_{i,j} < 0, \end{cases} \\
\beta_{i,j}^{(1)} &= \begin{cases} (c_\beta^+(\beta_{i,j}^{(0)} - l_\beta^+) + l_\beta^+)^{(+)} \text{ if } \beta_{i,j} \geq 0, \\ (c_\beta^-(\beta_{i,j}^{(0)} - l_\beta^-) + l_\beta^-)^{(-)} \text{ if } \beta_{i,j} < 0, \end{cases}
\end{aligned}
$$

where $c_l > 0, c_\alpha^+, c_\alpha^-, c_\beta^+, c_\beta^- > 0$ are the contrast parameters, $\tau^{(+)} = \max\{\tau, 0\}$, and $\tau^{(-)} = \min\{\tau, 0\}$.

Regarding the deblurring and denoising phase, in [11], the solution is defined through a regularization approach. In detail, a *clique* c of order 1 or 2 is a subset of points of a square grid on which the first or the second order finite difference is defined. Let C_1 be the set of all cliques of order 1 that is $C_1 = \{c = \{(i,j),(h,k)\} : i = h, j = k+1 \text{ or } i = h+1, j = k\}$; for the second order cliques we have that $C_2 = \{c = \{(i,j),(h,k),(r,q)\} : i = h = r, j = k+1 = q+2$ or $i = h+1 = r+2, j = k = q\}$). If $c = \{(i,j),(h,k)\} \in C_1$, then the first order operator is $D_c^1\mathbf{l} = l_{i,j} - l_{h,k}$, while if $c = \{(i,j),(h,k),(r,q)\} \in C_2$, then $D_c^2\mathbf{l} = l_{i,j} - 2l_{h,k} + l_{r,q}$. In [11], the second–order operators are used for restoring the luminance, while the first–order differences are used in the chrominance restoration. In the first order case, if $c = \{(i,j),(i+1,j)\}$, $i = 2,\ldots,M-1$, $j = 1,\ldots,N$, is a vertical clique its preceding clique is given by $c-1 = \{(i-1,j),(i,j)\}$. If $c = \{(i,j),(i,j+1)\}$, $i = 1,\ldots,M$, $j = 2,\ldots,N-1$, is a horizontal clique then its preceding clique is $c-1 = \{(i,j-1),(i,j)\}$. While, in second order case given $c = \{(i,j),(i+1,j),(i+2,j)\}$, $i = 3,\ldots,M-2$, $j = 1,\ldots,N$, we have $c-1 = \{(i-2,j),(i-1,j),(i,j)\}$, and for $c = \{(i,j),(i,j+1),(i,j+2)\}$, $i = 1,\ldots,M$, $j = 3,\ldots,N-2$, we have $c-1 = \{(i,j-2),(i,j-1),(i,j)\}$. [11] assumes that the blur matrix $A \in \mathbb{R}^{nm\times nm}$ that degrades the image is known.

Given a degraded luminance $\mathbf{l^{(1)}}$, the estimated solution $\mathbf{l^{(2)}}$ is the minimizer of the follow energy

$$E_1(\mathbf{l}) = \|A\mathbf{l} - \mathbf{l^{(1)}}\|^2 + \sum_{c \in C_2} \psi(D_c^2\mathbf{l}, D_{c-1}^2\mathbf{l}), \tag{1}$$

where

$$\psi(t_1, t_2) = \begin{cases} \lambda^2 t_1^2, & \text{if } |t_1| < s, \\ \theta, & \text{if } |t_1| \geq s, \end{cases} \quad \text{if } |t_2| < s, \\ \begin{cases} \lambda^2 t_1^2, & \text{if } |t_1| < \bar{s}, \\ \theta + \varepsilon, & \text{if } |t_1| \geq \bar{s}, \end{cases} \quad \text{if } |t_2| \geq s, \tag{2}$$

where $s = \sqrt{\theta}/\lambda$ and $\bar{s} = \sqrt{\theta + \varepsilon}/\lambda$. The first term of the energy E_1 in (Eq. 1) is related to the faithfulness of the solution to the data, while the second one is a smoothness condition on $\mathbf{l}$. The form of the function ψ in (Eq. 2), in addition to ensuring the presence of appropriate discontinuities in the reconstruction, allows the inhibition of adjacent parallel discontinuities (see also [14]). λ^2 is a regularization parameter that allows us to establish an appropriate degree of smoothness in the solution, $\theta \leq 0$ is the cost to introduce a discontinuity in the estimated luminance, while $\varepsilon \geq 0$ is the cost for parallel close discontinuities.

The energy E_1 is not convex, and thus [11] uses a GNC (*Graduated Non-Convexity*) algorithm to compute its minimizer. This algorithm is a deterministic technique that in the last years has had many applications in different fields (see, e.g., [12,14,18,23,26,27,38,40]). In particular, we use the GNC technique proposed in [13].

Moreover, [11] finds the chromatic estimate $(\boldsymbol{\alpha^{(2)}}, \boldsymbol{\beta^{(2)}})$ that minimizes the following energy.

$$\begin{aligned} E_2(\boldsymbol{\alpha}, \boldsymbol{\beta}) = \quad & \|A\boldsymbol{\alpha} - \boldsymbol{\alpha^{(1)}}\|^2 + \|A\boldsymbol{\beta} - \boldsymbol{\beta^{(1)}}\|^2 \\ & + \sum_{c \in C_1} \lambda^2 (D_c^1 \boldsymbol{\alpha})^2 + (D_c^1 \boldsymbol{\beta})^2)(1 - w_c). \end{aligned} \tag{3}$$

The faithfulness with data of the α- and the β-component of the chrominance are given by the first two terms of the energy E_2 in (Eq. 3). The third term is a regularizzation term, in which the line variables w_c, related to the discontinuity in the clique c, are given by the estimated luminance $\mathbf{l^{(2)}}$, namely $w_c = 1$ if there is a discontinity in $\mathbf{l^{(2)}}$; $w_c = 0$ otherwise. In this case, energy E_2 is convex. Thus, [11] computes the minimizer by a SOR-type algorithm.

3.1 Experimental Results of the First Phase

We now present some experimental results related to the defading phase. We examined the four 2000×1080 images in Fig. 5 (a). The choice of the examination cards is arbitrary but still such as to examine the different problems that arise in the reconstruction phase. We have implemented all the algorithms proposed

here in C language in a Linux environment. We estimate that the images were degraded by a blur matrix A derived from the following local blur mask.

$$M = \begin{pmatrix} 1 & 1 & 1 \\ 1 & 1 & 1 \\ 1 & 1 & 1 \end{pmatrix}$$

In [14], it is shown how to obtain the matrix A as a function of M. The parameters used in the color estimation phase are $l_0 = 100$, $c_l = 1.8$, $l_\alpha^+ = 0.4$, $c_\alpha^+ = 1.2$, $l_\alpha^- = -0.04$, $c_\alpha^- = 6$, $l_\beta^+ = 0.15$, $c_\beta^+ = 5$, $l_\beta^- = -0.004$, and $c_\beta^- = 5$; while the parameters used in the deblurring and denoising phase are $\lambda = 1$, $\theta = 200$, and $\epsilon = 200$. We have determined all these parameters through an experimental phase. The results obtained are presented in Fig. 5 (b).

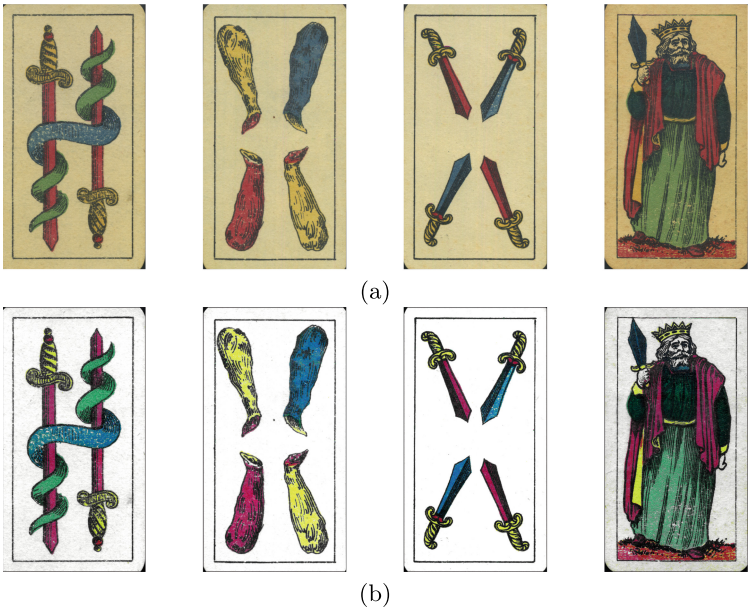

(a)

(b)

Fig. 5. The observed 2000×1080 images $x^{(0)}$; (b): The reconstructed image $x^{(2)}$.

4 Color Homogeneity Improvement Phase

After a phase in which the homogeneous color zones are clearly demarcated by black lines, we foresee a phase in which the homogeneity in these areas increases. Given an image $x^{(3)} = (\mathbf{l^{(3)}}, \boldsymbol{\alpha}^{\mathbf{(3)}}, \boldsymbol{\beta}^{\mathbf{(3)}}) \in \mathbb{R}^{n \times m \times 3}$, the black pixels are determined. Then, we define

$$C_1^* = \{c = \{(i,j),(h,r)\} \in C_1 : x_{i,j}^{(3)} \neq \textit{black} \text{ or } x_{h,r}^{(3)} \neq \textit{black}\}.$$

That is, C_1^* is the set of first-order cliques in $x^{(3)}$ that do not contain black pixels. Subsequently, starting from $x^{(3)}$, the minimizer $x^{(4)} = (\mathbf{l^{(4)}}, \boldsymbol{\alpha}^{(4)}, \boldsymbol{\beta}^{(4)})$ of the following energy function is determined.

$$E_3(x) = \sum_{c \in C_1^*} \left(\left(D_c^1 \mathbf{l}\right)^2 + \left(D_c^1 \boldsymbol{\alpha}\right)^2 + \left(D_c^1 \boldsymbol{\beta}\right)^2 \right).$$

The minimization of E_3 allows the areas delimited by the black lines to be almost uniform. This property is characteristic of card drawings, so we emphasize it in this phase. The energy E_3 is convex, so we use a SOR technique to minimize it.

4.1 Experimental Results of the Third Phase

The second phase, in which we construct black lines to delimit the homogeneous color areas, is done manually using the GIMP software. The results obtained from the images in Fig. 5 (b) are presented in Fig. 6 (a). Note that we have artificially added color to the king's skin to facilitate the subsequent reconstruction of the image. This color can be easily removed in the final restoration and does not compromise the integrity of the image. Moreover, the results obtained in the homogeneity increase phase are shown in Fig. 6 (b).

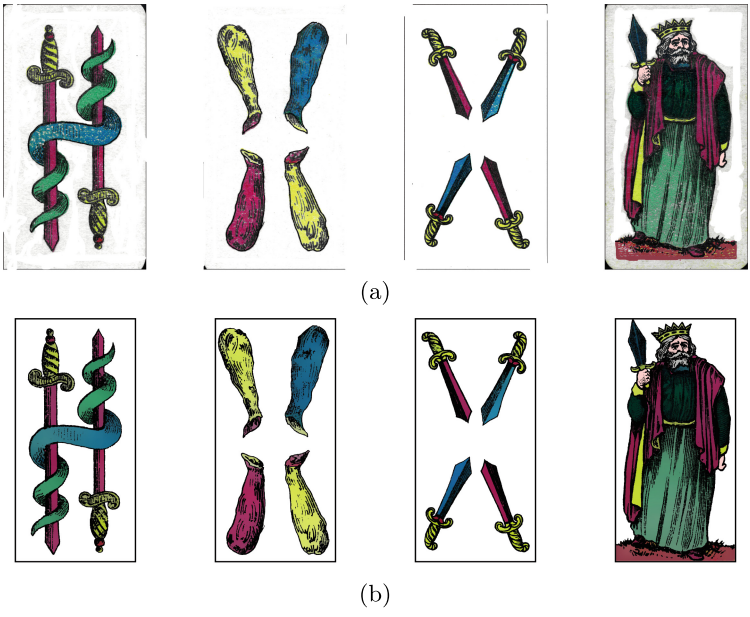

Fig. 6. (a): The data images $x^{(3)}$; (b): The reconstructed images $x^{(4)}$.

5 External Contour Detection

In this phase, we determine the external black contour. This phase is preparatory to the next one, where these contours will be regularized. We only deal with the external contours, as the internal ones are not easily distinguishable from black strokes. The colored strokes are part of the drawing and must be preserved not to diminish the card's artistic and artisanal contribution. Meanwhile, the external lines that delimit homogeneous areas are expected to be regular. Thus, irregularities in these lines are primarily due to printing inaccuracies and must be identified and eliminated. We have divided this phase into two sub-phases. The first of these is a quick reworking of the edge to eliminate the most visible imperfections. In particular, if on a row or column in the middle of white pixels, there are a number of consecutive black pixels less than a threshold t_1, then the black pixels are colored white. In this case, the black pixels are considered few to represent an edge. Similarly, if the number of white pixels in a row or column nested in black pixels is less than a threshold t_2, the white pixels are colored black. Also, if the number of black pixels followed by a colored pixel in a row or column is less than a threshold t_3, then the number of black pixels is increased until it reaches the threshold t_3.

In the second subphase, given the color image $x^{(5)} \in \mathbb{R}^{n \times m \times 3}$, an image $y^{(0)} \in \{white, black, colored\}^{n \times m \times 3}$ is obtained, where each pixel can assume three possible values: white, black, or colored. Subsequently, we examine all rows, all columns, and all diagonals along the directions $(1, 1)$, $(1, -1)$, $(1, 2)$, $(1, -2)$, $(2, 1)$, and $(2, -1)$. If there are black pixels between colored ones, the black pixels are considered colored. Such pixels are part of internal borders or colored patterns inserted into colored areas and, therefore, are not part of the external border.

5.1 Experimental Results of the Fourth Phase

In the first sub-phase, we empirically set the thresholds to $t_1 = 4$, $t_2 = 2$, and $t_3 = 8$. The obtained results are presented in Fig. 7 (a). The results related to the second sub-phase are shown in Fig. 7 (b).

6 External Contour Regularization

We now deal with regularizing the contour determined in the previous section. This contour presents irregular traits due to the imperfection of early twentieth-century printing. Thus, we impose regularization constraints. Regarding the consistency term with the data, we measure the difference between the result obtained and the one taken as given. We have divided the regularity term into two subterms. The first subterm measures the quantity of discontinuity elements in the reconstructed trichromatic image. However, this subterm could favor compact and thin black borders, so we have introduced a new subterm that constrains

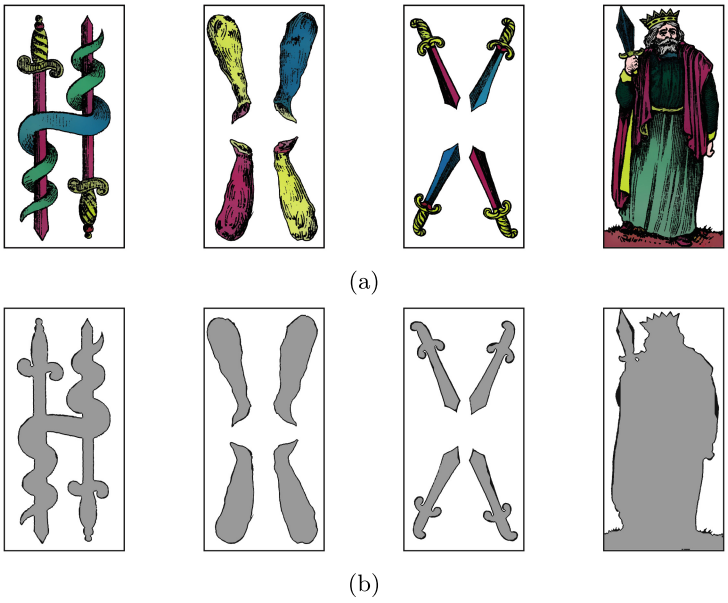

Fig. 7. (a): The restored images $x^{(5)}$; (b): The trichromatic images $y^{(0)}$.

the thickness of the black border to be, at most, equal to a predetermined constant.

In detail, let $y^{(0)} \in \{white, black, colored\}^{n\times m\times 3}$ be the given trichromatic image, and $y \in \{white, black, colored\}^{n\times m\times 3}$ be a generic trichromatic image, we define

$$D(y, y^{(0)}, i, j) = \begin{cases} d_1 & \text{if } y_{i,j} = white \text{ and } y^{(0)}_{i,j} = black, \\ d_2 & \text{if } y_{i,j} = white \text{ and } y^{(0)}_{i,j} = colored, \\ d_3 & \text{if } y_{i,j} = black \text{ and } y^{(0)}_{i,j} = white, \\ d_4 & \text{if } y_{i,j} = black \text{ and } y^{(0)}_{i,j} = colored, \\ d_5 & \text{if } y_{i,j} = colored \text{ and } y^{(0)}_{i,j} = white, \\ d_6 & \text{if } y_{i,j} = colored \text{ and } y^{(0)}_{i,j} = black, \\ 0 & \text{if } y_{i,j} = y^{(0)}_{i,j}, \end{cases}$$

where $d_i > 0$, $i = 1, \ldots, 6$ are positive weights to pay if they want to change a color from image $y^{(0)}$ to image y. Note that these values can differ depending on the configuration to be favored.

Given $c = \{(i, j), (h, r)\} \in C_1$ we define

$$E_c y = \begin{cases} e & \text{if } y_{i,j} \neq y_{h,r}, \\ 0 & \text{otherwise}, \end{cases}$$

where $e > 0$ is the cost to pay if there is a discontinuity in the clique c. Furthermore, let

$$L = \{(i,j) : y_{i,j} = colored\},$$

be the set of colored pixels, and let (i,j) be a pixel with $1 \leq i \leq n$ and $1 \leq j \leq m$ we define

$$\Delta(y,i,j) = \begin{cases} d((i,j),L) & \text{if } y_{i,j} = white \text{ and there exists a clique } c \in C_1 \\ & \text{such that } (i,j) \in c \text{ and } E_c y \neq 0, \\ 0 & \text{otherwise,} \end{cases}$$

where $d((i,j),L)$ is the Euclidean distance between the pixel (i,j) and the set L.

We thus define the regularized solution $y^{(1)}$ as the minimizer of the following energy function.

$$E_4(y) = \sum_{i=1}^{n}\sum_{j=1}^{m} D(y, y^{(0)}, i, j) + \sum_{c \in C_1} E_c y + \xi \sum_{i=1}^{n}\sum_{j=1}^{m} \Delta(y,i,j). \tag{4}$$

where $\xi > 0$ is a positive parameter that regulates the force we want to impose on the constraint of homogeneity of the border thickness.

Given the discrete nature of the energy function E_4 in (Eq. 4), finding an adequate convex approximation is not immediate. Thus, we minimized this function by a simulated annealing technique. In particular, we change the value of a pixel adjacent to a discontinuity at each iteration and evaluate the related change in energy. The configuration change is accepted in accordance with the simulated annealing technique.

6.1 Experimental Results of the Fifth Phase

We here consider as data the images in Fig. 7. We set the following parameters: $d_1 = d_3 = 20$, $d_2 = d_5 = 30$, $d_4 = d_6 = 0.5$, $e = 420$, and $\xi = 40$. We set the initial temperature of the annealing algorithm as $t = 1$, the temperature decay scheme as $t^{(i)} = 0.9 \cdot t^{(i-1)}$, the length of the Markov chains as $l = 100$, and the final temperature as $t = 0.02$. Figure 8 shows the obtained results.

7 Border Changing

In this section, given the image $x^{(5)} \in \mathbb{R}^{n \times m \times 3}$ with outer border $y^{(0)} \in \{white, black, colored\}^{n \times m \times 3}$ and the regularized outer border $y^{(1)} \in \{white, black, colored\}^{n \times m \times 3}$, we want to obtain a new image $x^{(6)} \in \mathbb{R}^{n \times m \times 3}$ with border $y^{(1)}$. Let $W^{(1)} = \{(i,j) : y^{(1)}_{i,j} = white\}$ be the set of new white pixels, $B^{(1)} = \{(i,j) : y^{(1)}_{i,j} = black\}$ be the set of new black pixels and $L^{(1)} = \{(i,j) : y^{(1)}_{i,j} = colored\}$ be the set of new colored pixels, and $L^{(0)} = \{(i,j) : y^{(0)}_{i,j} = colored\}$ be the set of colored pixels in $y^{(0)}$. If $(i,j) \in W^{(1)}$ then we impose that $x^{(6)}_{i,j}$ to be white, if

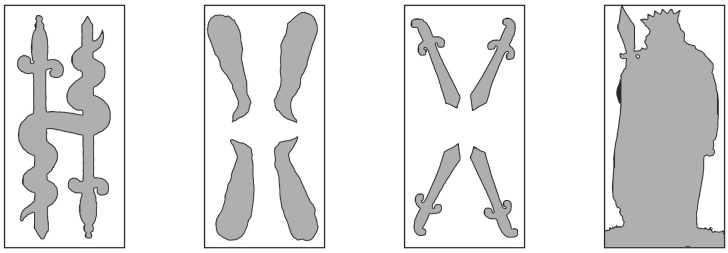

Fig. 8. The regularized trichromatic images $y^{(1)}$.

$(i,j) \in B^{(1)}$ then we impose that $x_{i,j}^{(6)}$ to be black. If $(i,j) \in L^{(1)} \cap L^{(0)}$ then we set $x_{i,j}^{(6)} = x_{i,j}^{(5)}$.

We made a special treatment for pixels such that $(i,j) \in L^{(1)} \setminus L^{(0)}$. We determine their intensity through a regularization technique. In order to reduce the computational costs, we initialize such pixels as follows. A pixel $(i,j) \in L^{(0)}$ in the image $x^{(5)}$ could be either black or colored. So let $L_x = \{(i,j) : (i,j) \in L^{(0)}$ and $x_{i,j}^{(5)}$ is colored$\}$ be the set of pixels that are not part of the external border that are colored in $x^{(5)}$, and $B_x = \{(i,j) : (i,j) \in L^{(0)}$ and $x_{i,j}^{(5)}$ is black$\}$ be the set of pixels that are not part of the external border but are black in $x^{(5)}$. Given a pixel $(i,j) \in L^{(1)} \setminus L^{(0)}$, if it has more adjacent pixels in B_x than in L_x, then we impose $x_{i,j}$ to be black. Otherwise, we set $x_{i,j}$ to be the average of the color intensities of the adjacent pixels in L_x. In this way, we avoid creating color shades not present in the ideal image to be reconstructed.

Let us define the following subset of cliques.

$$C_1^{\#} = \{c = \{(i,j),(h,r)\} \in C_1 : (i,j) \in L^{(1)} \setminus L^{(0)} \text{ and } (h,r) \notin B^{(1)}\}.$$

The estimated solution $x^{(6)} = (\mathbf{l^{(6)}}, \boldsymbol{\alpha^{(6)}}, \boldsymbol{\beta^{(6)}})$ is the minimizer of the follow energy.

$$E_5(x) = \sum_{c \in C_1^{\#}} \psi(D_c^1 x, D_{c-1}^1 x), \tag{5}$$

where the function ψ is as in (Eq. 2), and

$$D_c^1 x = \sqrt{D_c^1 \mathbf{l} + 255(D_c^1 \boldsymbol{\alpha} + D_c^1 \boldsymbol{\beta})}.$$

Note that we have multiplied the chrominance terms by 255 to ensure that these terms have the same size as the luminance terms. The problem examined in this section is known in the literature as sparse data reconstruction (see also [20]). We use the GNC technique proposed in [13] to minimize the energy function E_5 in (Eq. 5).

7.1 Experimental Results of the Sixth Phase

We have set the regularization parameters in (Eq. 2) to $\lambda = 4$, $\theta = 20000$, and $\epsilon = 10000$. Given the images in Fig. 7 (b) and the new border in Fig. 8, we obtained the reconstructed images in Fig. 9.

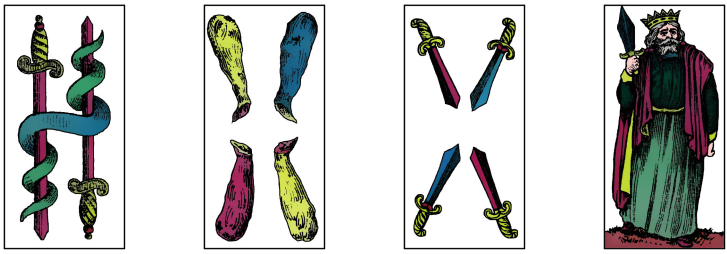

Fig. 9. The reconstructed images $x^{(6)}$.



(a) (b) (c)

Fig. 10. (a): Greek playing cards produced by Aspioti–ELKA (from Gerace's private collection); (b): *Minchiate* playing cards (from Gerace's private collection); (c) *Napoletane* playing cards produced by Pignalosa (from Gerace's private collection).

Conclusions

In this paper, we analyzed the study of the digital reconstruction of ancient playing cards. We divided the reconstruction into several phases. In particular, we

analyzed the balancing and homogenization of the color, the finding and regularization of the external contour, and the final adaptation of the data. We proposed different regularization techniques to solve the various problems. In particular, innovative smoothness terms were proposed for regularizing the external contour. Experimental results have confirmed the validity of these techniques.

In the future, we intend to complete the automatic resolution of this problem with a phase of closing the external border and an anti-aliasing final phase [37]. We also foresee the reconstruction of several historically important decks of cards such as the Greek deck with Italian suits produced by Aspioti–ELKA (Fig. 10 (a)), the deck of Tuscan *Minchiate* cards (Fig. 10 (b)), or a deck of ancient *Napoletane* playing cards (Fig. 10 (c)).

Acknowledgement. We want to thank the *Associazione 7bello - Cartagiocofilia Italiana A.P.S.* for the support and suggestions given, and in particular to Nicola Antonio De Giorgio. We also thank Virgilio Ferrari for providing the images of the deck of cards under reconstruction. This work is supported by PRIN 2022 – Prot. 2022S5LET5 "The textual legacy of the Ostrogoths in Italy: The Bible version and other texts".

References

1. Annuario d'Italia. Stabilimento Tipo–Litografico dell'Annuario d'Italia, Genova (1889)
2. Annuario d'Italia. Stabilimento Bontempelli, Roma–Genova (1892)
3. Annuario d'Italia. Stabilimento Bontempelli, Roma–Genova (1893)
4. Annuario d'Italia. Stabilimento Bontempelli, Roma–Genova (1894)
5. Annuario d'Italia. Stabilimento Bontempelli, Roma (1896)
6. Annuario d'Italia. Stabilimento Bontempelli, Roma (1899)
7. Ahmed, A. M. T.: Color restoration techniques for faded colors of old photos, printings, and paintings. In: Proceedings of 2009 IEEE International Conference on Electro/Information Technology, pp. 151–156 (2009)
8. Associazione 7bello – Cartagiocofilia Italiana A.P.S. https://www.7bellonline.it/. Accessed 20 Mar 2025
9. Barzegar Khalilsaraei, S., Komar, A., Zheng, J., Augsdörfer, U.: InceptCurves: curve reconstruction using an inception network. Vis. Comput. **40**, 4805–4815 (2024)
10. Basova, O., et l.: Uniform color space with advanced hue linearity: PCS23-UCS. In: Schettini, R., Trémeau, A., Tominaga, S., Bianco, S., Buzzelli, M. (eds.) Computational Color Imaging. CCIW 2024. LNCS, vol. 15193. Springer, Cham. (2025). https://doi.org/10.1007/978-3-031-72845-7_3
11. Biondi, G., Boccuto, A., Gerace, I.: Quadratically transformed luminance chrominance spaces. In: Gervasi, O., et al. Computational Science and its Applications – ICCSA 2023 Workshops. ICCSA 2023. LNCS, vol. 14108. Springer, Cham, pp 676–693 (2023). https://doi.org/10.1007/978-3-031-37117-2_45
12. Boccuto, A., Gerace, I., Giorgetti, V.: A graduated non-convexity technique for dealing large point spread functions. Appl. Sci. **2**(10), 28 (2023)
13. Boccuto, A., Gerace, I., Giorgetti, V., Martinelli, F., Tonazzini, A.: An edge-preserving regularization model for the demosaicing of noisy color images. J. Math. Imag. Vis. **66**, 904–925 (2024)

14. Boccuto, A., Gerace, I., Martinelli, F.: Half-quadratic image restoration with a non-parallelism constraint. J. Math. Imag. Vis. **59**(2), 270–295 (2017)
15. Bruni, V., Ramponi, G., Restrepo, A., Vitulano, D.: Context-based defading of archive photographs. EURASIP J. Image Video Process. **2009**, 986183, 11 (2009)
16. De Giorgio N.A.: La manifattura delle carte da gioco di Guglielmo Murari. Comune di Veglie (2005)
17. Demoment, G.: Image reconstruction and restoration: overview of common estimation structures and problems. IEEE Trans. Acoust., Speech Sig. Process. **37**, 2024–2036 (1989)
18. Evangelopoulos, X., Brockmeier, A. J., Mu, T., Goulermas, J. Y.: A Graduated non-convexity relaxation for large-scale seriation. In: Proceedings of the 2017 SIAM International Conference on Data Mining, Houston, Texas (USA), pp. 462–470 (2017)
19. Fairchild, M.D.: Color and Image Appearance Models. Wiley, Color Appearance Models (2005)
20. Gerace, I., Palomba, C., Tonazzini, A.: An inpainting technique based on regularization to remove bleed-through from ancient documents. In: Proceedings of the 2016 International Workshop on Computational Intelligence for Multimedia Understanding (IWCIM), Reggio Calabria, Italy, pp. 1–5 (2016)
21. Guilmeau, T., Chouzenoux, E., Elvira, V.: Simulated annealing: a review and a new scheme. In: Proceedings of the 2021 IEEE Statistical Signal Processing Workshop (SSP), Rio de Janeiro, Brazil, pp. 101–105 (2021)
22. Hargrave, C.P.: An History of Playing Cards. Courier Corporation, United States (2014)
23. Hazan, E., Levy, K. Y., Shalev-Shwartz, S.: On graduated optimization for stochastic non-convex problems. In: Proceedings of the 33rd International Conference on Machine Learning, New York, NY, USA, 2016. JMLR: W& CP, vol. 48, pp. 1–9 (2016)
24. Jilley, R.: A History of Playing cards. Studio Vista, London (1973)
25. Laville, B., Blanc-Féraud, L., Aubert, G.: A Γ-convergence result and an off-the-grid charge algorithm for curve reconstruction in inverse problems. J. Math. Imag. Vis. **66**, 572–583 (2024)
26. Kang, W., Kim, J., Chung, J., Choi, S., Kim, T.-W.: Improving pose graph optimization via efficient graduated non-convexity scheduling. Int. J. Control Autom. Syst. **23**, 405–417 (2025)
27. Liu, Z.-Y., Qiao, H.: GNCCP-graduated NonConvexity and concavity procedure. IEEE Trans. Pattern Anal. Mach. Intell. **36**(6), 1258–1267 (2014)
28. Mann, S.: Alle Karten auf den Tisch: Geschichte der standardisierten Spielkarten aller Welt - All cards on the table: Standard Playing Car. Jonas-Verlag, Deutsches Spielkarten-Museum (Leinfelden-Echterdingen) (1990)
29. Mann, S.: Collecting Playing Cards. Howard Baker Press (1966)
30. Nikitenko, D., Wirth, M., Trudel, K.: Applicability of white-balancing algorithms to restoring faded colour slides: an empirical evaluation. J. Multimedia **3**(5), 9–18 (2008)
31. Restrepo, A., Ramponi, G.: Filtering and luminance correction for aged photographs. In: Image Processing: Algorithms and Systems VI, Proceedings of SPIE, vol. 6812, pp. 26–31, San Jose, Calif, USA (2008)
32. Panetta, K.A., Wharton, E.J., Agaian, S.S.: Human visual system-based image enhancement and logarithmic contrast measure. IEEE Trans. Syst. Man Cybern. **38**(1), 174–188 (2008)

33. Pratesi, F.: Notturno's Gioco di Triomphi. Playing-Card **17**(1), 23–33 (1988)
34. Pratesi, F.: 1510ca: Assisi – Mazzo completo di 48 carte, naibi.net, p. 14 (2016). https://www.naibi.net/A/601-UMBRIA-Z.pdf
35. Pratesi, F.: Il terzo foglio Rosenwald, naibi.net, pp. 15 (2016). https://www.naibi.net/A/516-ROSEN3-Z.pdf
36. Pratesi, F.: Carte da Perugia e cittá vicine, naibi.net, p. 14 (2017). https://www.naibi.net/A/601-UMBRIA-Z.pdf
37. Sabry, F.: Anti Aliasing: Enhancing Visual Clarity in Computer Vision. One Billion Knowledgeable, (2024)
38. Smith, T., Egeland, O.: Dynamical pose estimation with graduated non-convexity for outlier robustness. MIC—Model. Identif. Control **43**(2), 79–89 (2022)
39. Tarot-as-Tarocchi. https://www.tarot-as-tarocchi.com/files/piacentine-perugia-1.jpg. Accessed 7 Mar 2025
40. Yang, H., Antonante, P., Tzoumas, V., Carlone, L.: Graduated non-convexity for robust spatial perception: from non-minimal solvers to global outlier rejection. IEEE Robot. Autom. Lett. **5**(2), 1127–1134 (2020)